The effect of tree decline over soil microclimate largely controls soil respiration dynamics in a Mediterranean woodland

Authors: Alexandra Rodríguez[1]*, Jorge Durán[1,2], Jorge Curiel Yuste[3,4], Fernando Valladares[5,6,7], Ana Rey[5]

*Corresponding author

[1]Centre for Functional Ecology, CFE, University of Coimbra, 3000-456 Coimbra, Portugal

[2]Misión Biolóxica de Galicia, Consejo Superior de Investigaciones Científicas, 36143 Pontevedra, Spain

[3]BC3 - Basque Centre for Climate Change, Scientific Campus of the University of the Basque Country, 48940 Leioa, Spain

[4]IKERBASQUE - Basque Foundation for Science, Maria Diaz de Haro 3, 6 solairua, 48013 Bilbao, Bizkaia, Spain

[5]Department of Biogeography and Global Change, National Museum of Natural Sciences, MNCN, CSIC, 28006 Madrid, Spain

[6]LINCGlobal, Madrid, Spain

[7]Area of Biodiversity and Conservation, ESCET, Rey Juan Carlos University, 28933 Móstoles, Madrid, Spain

Present postal address of the corresponding author:

Centre for Functional Ecology, CFE, Department of Life Sciences, University of Coimbra, Calçada Martim de Freitas, 3000-456 Coimbra, Portugal

Full telephone: +351 239240752; E-mail: arp@uc.pt

Type of article: Research paper.

Abstract

As drought-induced tree defoliation and mortality (i.e. tree decline) in the Mediterranean is expected to worsen with ongoing climate change, it is of paramount importance to understand how, why, and when tree decline affects soil respiration (R_s) and its relationship with soil microclimate and other potential controls. We carried out a novel study exploring the interacting effects of climatic variability and tree decline on soil microclimate and R_s temporal variability in a Mediterranean holm oak woodland. The study further explores the effects of tree decline on the main controls of R_s at the stand scale. We monitored R_s, soil temperature (T_{soil}), and soil volumetric water content (SWC) under the canopy of 30 holm oak trees with different defoliation degrees (healthy, affected, and dead) during two years of contrasting precipitation patterns. We estimated different plant structural variables (e.g. DBH, height, and canopy diameter) on those selected trees under whose canopies we also collected soil samples to analyze different soil physicochemical variables. Our results stress the important role of tree health as a modulator of the response of R_s to SWC, with stronger responses of R_s to variations in the amount and distribution of precipitation under healthy than under declining trees. They also suggest that tree decline can significantly increase SWC and decrease R_s but largely depending on the declining stage, the year, and the season. Finally, tree decline also affected the relationship of R_s with soil microclimatic variables, particularly SWC, and the relative importance of the different drivers of R_s, with microclimate variables gaining importance as trees defoliate and die. Altogether, our results point towards a negative impact of drought-induced tree decline on soil C content and cycling, particularly under forecasted climate change scenarios with dryer and more intense precipitation regimes.

Keywords: *Quercus ilex*; forest die-off; climate change; soil functioning; soil CO_2 efflux; environmental control.

1. Introduction

Climate models in Mediterranean ecosystems forecast increases in temperature and more intensive and extensive droughts, with more frequent and intense extreme temperature and precipitation events (IPCC, 2021). These changes will affect the structure, composition, and functioning of forests in still unknown ways, with important implications for the carbon (C) balance (Liu et al., 2016; Reichstein et al., 2013; Wang et al., 2012). Forecasted changes in the frequency, intensity, and distribution of rainfall events (IPCC, 2021) will likely increase the importance of rainfall pulses on the C cycle of Mediterranean environments (Rey et al., 2021, 2017; Song et al., 2017; Wang et al., 2016), largely influenced by the intra-annual variation in soil water content (Gallardo et al., 2009). Also, the increasingly dry and hot climatic conditions will exacerbate the drought-induced tree defoliation and mortality (hereinafter "forest die-off") observed over the past two decades (Carnicer et al., 2011; Lloret et al., 2004).

Drought-induced forest die-off impacts forest ecosystems by reducing tree productivity, reducing the input of litter and root exudates, and modifying soil microclimatic conditions, and in turn, soil microbial communities (Schlesinger et al., 2016). Accordingly, Rodríguez et al. (2017, 2020) found evidence of a cascade effect of ongoing drought-induced forest die-off in a Mediterranean holm oak (*Quercus ilex*) woodland ultimately decreasing the content and lability of soil C. Although efforts to understand the effects of forest die-off on important soil processes related to C cycling have increased lately (Avila et al., 2019, 2016; Curiel Yuste et al., 2019; García-Angulo et al., 2020), results are still scarce and contradictory. For instance, some studies have reported decreases in soil respiration (R_s) as a result of reduced root activity (Avila et al., 2016), whereas others have found no changes (Barba et al., 2016) or even increased rates (Barba et al., 2013; Curiel Yuste et al., 2019; Edburg et al., 2012) following changes in microclimate (e.g., increases in soil moisture), increasing litter inputs and secondary successional processes. Thus, the impacts of forest die-off on R_s are complex and

largely depend on the balance of its effects on roots (autotrophic) and microbial (heterotrophic) components (Avila et al., 2016). Moreover, recent studies suggest that forest die-off can largely modulate the response of microbial respiration to climate change and that forest die-off effects on different soil attributes and processes are seasonal (Avila et al., 2019, 2016; Rodríguez et al., 2019). Still, the interacting effects of tree decline and climatic variability on R_s have been scarcely explored, specifically considering Mediterranean forests and drought as the main driver of tree decline (Barba et al., 2016).

Soil respiration is the largest source of CO_2 from terrestrial ecosystems and, therefore, a central piece of the global C balance (Schlesinger and Andrews, 2000). However, it is also a very complex process controlled by several physiological, phenological, and environmental processes that vary both in time and space (Rey et al., 2021, 2011; Tang and Baldocchi, 2005). At the global scale, its temporal and spatial variability is mainly controlled by air temperature and precipitation, whereas at micro and stand scales, other factors related to plant community and soil organic matter become more important (Barba et al., 2013; Raich and Schlesinger, 1992). Moreover, whereas autotrophic respiration (R_A) is mainly controlled by tree physiology and productivity (Högberg et al., 2001; Matteucci et al., 2015), heterotrophic respiration (R_H) is largely controlled by soil microclimatic (i.e. water content and temperature) and biogeochemical factors (e.g. organic matter content and quality, microbial community structure) (Curiel Yuste et al., 2007; Tang and Baldocchi, 2005; Zhao et al., 2016). This complexity is at least partially responsible for the large uncertainties associated with predictions of global rates of R_s and R_s responses to climate change (Warner et al., 2019). Thus, there is an urgent need to continue to study this critical ecosystem process under different scenarios and at different temporal and spatial scales.

We carried out a novel two-year field study to explore the interacting effects of climatic variability and different stages of tree decline (i.e. healthy, affected, and dead) on soil

microclimate and R_s in a *Quercus ilex* Mediterranean woodland. Furthermore, we explored the effects of tree decline alone on the main controls of R_s at the stand scale (i.e. plant variables and soil microclimatic and physicochemical variables). We hypothesized that i) tree decline modifies soil microclimatic conditions and, in turn, R_s rates, but ii) these effects would depend on the season and year. Moreover, assuming changes in the relative contribution of R_A and R_H associated with tree decline (Curiel Yuste et al., 2019), we hypothesized that iii) the relative importance of plant, soil microclimatic, and physicochemical variables controlling R_s would change considering all tree decline stages (i.e. healthy, affected and dead) together and separately.

2. Material and Methods

2.1 Study site

The study was carried out in a holm oak woodland located in the central part of the Iberian Peninsula, southwest of Madrid (40°23′N, 4°11′W; 630-660 m above sea level). The climate is continental Mediterranean with mean annual temperature of 13 °C and mean annual precipitation of 601 mm (Felicísimo et al., 2011). Most rainfall concentrates from autumn to spring, while summers are warm and dry. Soil is a Cambisol, sandy and slightly acid (pH~6.3), with low total C and N content (Table S1). Aboveground vegetation is characterized by a tree density of ~180 trees ha^{-1}, mostly composed of *Quercus ilex L.* ssp. *ballota* [Desf.] Samp (holm oak) with scarce *Juniperus oxycedrus* Sibth. & Sm (cedar). The understory is dominated by *Retama sphaerocarpa* L., *Lavandula stoechas* ssp. *pedunculata* (Mill.) Samp. ex Rozeira, and diverse pasture species (Rodríguez et al., 2017). In 2005, this region suffered a strong event of holm oak defoliation (around 20–30% of the total population) and mortality (15%) due to a severe drought. Since then, the holm oaks of this woodland show different decline stages

(healthy, affected, and dead) with contrasting soil attributes underneath (Rodríguez et al., 2020, 2017) (Table S1).

2.2 Experimental design

In spring 2013, we selected 30 holm oak adult trees of similar size (38 cm and 4 m of diameter at breast height and height on average, respectively, Table S1) but with different levels of canopy decline (10 healthy, 10 affected, and 10 dead), and consequently with significantly different canopy diameter (Table S1; Rodríguez et al. 2017), separated at least 10 m from other trees. Canopy decline status of the different trees was visually determined – *healthy* <10% defoliated; *affected* > 50% defoliated; *dead* 100% defoliated.

On the north face of each tree, we established a sampling point below the influence of the tree canopy, 0.3 m away from the trunk (Rodríguez et al., 2017). Then polyvinylchloride soil collars (15 cm in diameter and 7 cm in height) were inserted 3.5 cm into the soil at each sampling point, where they remained for two consecutive annual periods: from June 2013 to May 2014 (*year 1*) and from June 2014 to May 2015 (*year 2*).

Both annual periods were extremely warm according to the reference period (1971-2000 and 1981-2010 until and from January 2015, respectively; AEMET), with similar mean annual air temperatures (15.9 ^{o}C and 15.8 ^{o}C, respectively) but lower precipitation values in *year 1* (288.8 mm) than in *year 2* (343.3 mm), particularly in late summer and fall (Fig. 1).

2.3 Soil microclimate and soil respiration measurements

We monitored R_s, along with soil temperature (T_{soil}) and soil volumetric water content (SWC), in all sampling points from June 2013 to May 2015 at a frequency of approximately twice a month during spring and fall and once a month during summer and winter (30 campaigns in total; Figure 1). To avoid strong diurnal fluctuations, measurements were done during the

midday period (between 10:00 and 14:00 h). Moreover, special care was taken to fully randomize the sampling sequence across tree decline stages in each measurement campaign. Small plants, excessive litter, insects, and grasses were carefully removed from each collar before each R_s measurement. A portable infrared gas analyzer (IRGA) connected to a soil respiration chamber (EGM-4 and SRC-1; PP Systems, USA) was used to measure R_s rates in situ during 90 s to ensure reliable measurements. At the time of each R_s measurement, T_{soil} and SWC were also measured adjacent to each soil collar at 4 cm depth (the most active) inserting vertically a soil digital thermometer (Maxtech, Lokhnath Enterprise, India) and a time-domain reflectometer (Fieldscout TDR 300, Spectrum Technologies, Inc., Plainfield, IL, USA), respectively. We estimated seasonal, annual, and two-year average values of R_s, T_{soil}, and SWC considering all measures carried out within each respective period. Whereas our experimental design hardly provides accurate daily, seasonal or annual R_s estimations, it is perfectly valid in terms of comparison among the different decline stages and correlations with the different predictor variables.

2.4 Plant and soil physicochemical variables

At the end of May 2013, we measured tree height, diameter at breast height (DBH), and the canopy diameter of the 30 studied trees by using a clinometer, a DBH tape, and averaging two perpendicular measurements of canopy diameter, respectively. We also estimated a distance-dependent competition index between trees for each one of the studied trees (Hegyi 1974), considering all the competing holm oaks and cedars within a 5.5 m radius, the DBH of the subject tree and that of its competitors as well as the distance between the subject tree and its competitors (Table S1; Rodríguez et al. 2017). On the same date, we also measured soil compaction in all sampling points by using a soil compaction meter (FieldScout SC 900, USA).

We carried out two different soil samplings (May 2013 and March 2015) to estimate various physicochemical variables for each decline stage (healthy, affected, and dead). Soil samples were collected close to the soil collars and from the first 10 cm of the soil profile by using a 5 cm (i.d.) metal corer and then kept at 4 °C until analysis. Before analysis, soil samples were sieved (2 mm mesh size), homogenized in field-moist conditions and analyzed for gravimetric moisture by oven-drying a subsample at 60 °C to constant mass. Soil total C and N content, and soil pH, were analyzed in soil samples collected in May 2013 by dry combustion with an elemental analyzer (LECO TruSpec CN, St. Joseph, MI, USA) and using a soil-to-water ratio of 1:2.5 (m/v), respectively. The possible occurrence of inorganic C was checked by a Dietrich-Fruhling volumetric calcimeter. Given its absence, total C was considered equal to soil organic C. Labile C was determined in the 2015 samples by using the High Gradient Magnetic Separation (HGMS) method as described in Rodríguez et al. (2020). Briefly, 10 grams of each sample underwent HGMS by a Frantz Isodynamic Separator (Model L-1, SG Frantz Co, Inc., Trenton, New Jersey, USA) that separated each soil sample in two fractions with different turnover times, a non-magnetic and a magnetic fraction (Chiti et al., 2019). The magnetic fraction has larger contributions from relatively recent C forms than the non-magnetic fraction and thus, is supposed to be more labile. We analyzed total C in the MA fraction (C_{MA}) by dry combustion (see above) and considered it as labile C. Soil bulk density was also estimated in the soil samples collected in 2015 (Table S1).

2.5 Statistical analyses

Linear models were performed to relate seasonal air temperature and precipitation values with our estimated T_{soil} and SWC seasonal values, respectively, as indicative of the suitability of our seasonal measurements.

We used generalized least squares (GLS) models to test the effects of soil microclimatic (inter- and intra-annual) variability and tree decline status, as well as their interactions, on SWC, $T_{soil,}$ and R_s. Pairwise statistical differences among the means of the factor levels were tested using simultaneous tests for general linear hypotheses (multiple comparisons of means: Tukey contrasts). For all the GLS models, the tree was used as a random factor to account for temporal dependencies and, when necessary, no-normality and heteroscedasticity of the residuals were corrected by log-transforming the dependent variable and/or using the argument weights, respectively.

We explored the relationship between R_s and T_{soil} for the whole sampling period and each decline stage separately using averaged values for each temperature degree. We identified two different periods determined by a temperature threshold from which the relationship of R_s with T_{soil} changes (Period I – below the temperature threshold, most of the year except summer; and Period II –from the threshold, summer). For Period I, soil respiration was considered dependent on soil temperature according to an exponential relationship:

$$R_s = R_{basal} * e^{b * T} \quad (1)$$

where R_s is the soil respiration (µmol C m^{-2} s^{-1}), T is soil temperature (ºC) measured at a depth of 4 cm, and R_{basal} (the basal respiration rate) and b are fitted parameters. The Q_{10} (the increase in the flux rate for a 10 ºC increase in temperature) was calculated as follows:

$$Q_{10} = e^{10 * b} \quad (2)$$

For Period II, R_s was better explained by soil water content through a logarithmic function:

$$R_s = a + b * ln(SWC) \quad (3)$$

where SWC (%) is soil volumetric water content measured at the depth of 4 cm, and *a* and *b* are fitted parameters.

We then used a multimodel inference approach based on information theory and ordinary least-squares (OLS) regressions to evaluate the relative importance of plant (canopy diameter) and soil microclimatic (two-year average values of T_{soil} and SWC) and physicochemical (C_{MA}, TN, bulk density) variables on the two-year average values of R_s for all decline stages together and separately (Burnham and Anderson, 2010). These variables were selected based on their ecological importance to the ecosystem functioning, its relationship with R_s and their independence from each other (Figure S1, supplementary material). Canopy diameter was shown to be significantly affected by tree defoliation degree (Table S1; Rodríguez et al. 2017) and thus considered as a surrogate of tree decline status ($R^2_{adj} = 0.30$, $P < 0.01$).

We used R 3.6.1 (R Core Team, 2017) for GLS models (nlme; Pinheiro et al., 2020), multiple comparisons between the means of the factor levels (multicomp; Bretz et al., 2011) and spearman correlations between our different variables (corrplot; Taiyun and Simko, 2017). Also, we used SigmaPlot 14.0 (Systat Software, San Jose, CA) for the relationships between soil respiration and the soil microclimatic variables, and SAM 4.0 (Rangel et al., 2010) for the multimodel inference approach.

3. Results

Similar to air temperature and precipitation, T_{soil} and SWC showed large and opposed ($\rho = -0.70$, $P < 0.001$) seasonal dynamics typical of the Mediterranean climate (Fig. 1; Table S2). Despite the limited and irregular number of T_{soil} and SWC measurements per season and year, our estimated seasonal values for these two microclimatic variables were largely explained by seasonal air temperature (75%) and precipitation (87%), respectively ($P < 0.001$).

3.1 Interacting effects of year, season and tree decline on soil microclimate and R_s

Both years showed similar annual means (18 °C and 17.7 °C, respectively) and seasonal dynamics (Fig. 1; Table 1 and S2) of T_{soil}. On the contrary, annual means of SWC were significantly lower (43%) in *year 1* than in *year 2* (Table 1), and whereas the minimum SWC values of both years occurred in mid-summer (~ 0.1 %), maximum values were found in winter for *year 1* (15%) and in autumn for *year 2* (22%; Fig. 1, Table S2). Similarly, R_s was significantly lower in *year 1* than in *year 2* (2.37 vs. 2.72 μmol C m^{-2} s^{-1}, respectively; Table 1) and showed a significant "year x season" interaction tightly linked to the different seasonal dynamics (intra-annual variability) of SWC for both years (Table S2). Thus, while in *year 1*, R_s picked in spring and showed the lowest values in fall, in *year 2*, R_s picked in fall and showed the lowest values in winter (Figure 1, Table S2). Consequently, seasonal means of R_s were 68% lower in *fall 1* than in *fall 2*, but 70% higher in *winter 1* than in *winter 2* (Table S2). The above-described differences in SWC between years and among seasons were independent of the defoliation degree. However, in the case of R_s, we found a significant "decline status x year" interaction with annual means significantly higher (22%) in *year 2* than in *year 1* under healthy but not under affected (5%) and dead (16%) trees (Table 1).

Considering the whole studied period, T_{soil} ranged between 5–34 °C, 4–37 °C and 5–41 °C under healthy, affected and dead trees, respectively, with similar average values (~18°C) under all decline stages. Thus, although the maximum T_{soil} values increased with defoliation degree, we found neither a significant overall effect of tree decline nor a significant decline status x year interaction on T_{soil} (Table 1). However, we did find a significant "decline status x season" interaction on T_{soil} of *year 2*, with significantly higher values under healthy than under dead trees in fall (Table 2). In the case of SWC, tree decline had a significant overall and positive effect, with significantly higher SWC values under dead (6.1% on average) than under

healthy (4.3%), and intermediate values under affected (5.6%; Table 1) trees. These differences were independent of the year but not of the seasonality, as neither *winter 2* nor any of the summers showed those differences among decline stages (Table 2). Finally, considering the whole studied period, R_s ranged between 0.39-9.22, 0.07-6.02, and 0-7.51 μmol C m^{-2} s^{-1} under healthy, affected and dead trees, with average values of 2.96, 2.14 and 2.54 μmol C m^{-2} s^{-1} respectively. Although we did not find a significant overall effect of tree decline on R_s, we did find a significant "decline status x year" interaction, with values 48% and 19% higher under healthy than under affected and dead trees, respectively, in *year 2* ($P < 0.001$; Table 1). These differences were observed in all seasons, except in spring (Table 2). Moreover, in *year 1* we found a significant "decline status x season" interaction, with R_s values in summer and winter up to 111% higher under healthy than under declining trees (Table 2). When expressing R_s on a C basis, we also obtained a significant "decline status x year" interaction with a trend (not significant) to lower values under affected (14% and 33% for *year 1* and *2*, respectively) and dead (15% and 17% for year 1 and 2, respectively) than under healthy trees (Table 1).

3.2 Tree decline modulates the relationship between R_s and soil microclimatic variables

Based on the differences found among tree decline stages above discussed, R_s was modelled as a function of T_{soil} and SWC for each decline stage separately. Moreover, as explained in the Methods section, we identified two different periods determined by a T_{soil} threshold (17 ºC for healthy and dead and 18 ºC for affected trees), below (Period I) and above (Period II) which R_s was considered dependent on T_{soil} and SWC, respectively (Fig. S2, Supplementary material). Those temperature thresholds corresponded to SWC values of 4%, 5% and 7% for healthy, affected and dead trees, respectively. Period I mostly corresponded to fall, winter and spring microclimatic conditions, whereas Period II mostly corresponded to summer conditions.

297 During Period I, R_s related to T_{soil} through an exponential relationship that explained
298 the 72%, 91% and 75% of the variance for healthy, affected and dead trees, respectively, and
299 with values of basal respiration of 1.053 (SE 0.221), 0.662 (SE 0.089) and 0.832 (SE 0.177)
300 μmol C m^{-2} s^{-1}, and Q_{10} values of 2.16, 2.48 and 2.32 (Fig 2a, 2b, and 2c). During Period II,
301 R_s was related to SWC through a logarithmic function, explaining 18%, 69% and 56% of the
302 variance for healthy, affected and dead, respectively (Fig 2d, 2e, and 2f). These results point
303 out tree decline status as a modulator of the relationship of R_s with soil microclimatic variables,
304 and particularly with SWC, suggesting a higher control of R_s by SWC under affected and dead
305 trees than under healthy trees. Accordingly, we also found a significant relation between the
306 seasonal means of R_s and those of precipitation under affected ($\rho = 0.81$, $P < 0.05$) and dead (ρ
307 $= 0.83$, $P < 0.05$) trees but not under healthy trees ($\rho = 0.69$, $P = 0.07$).
308
309 *3.3 Tree decline changes the relative importance of the main drivers of soil respiration*
310 The multimodel inference approach revealed that canopy diameter (surrogate of tree decline
311 status) and soil total N were the most important predictors for the two-year average values of
312 R_s considering all decline stages together (Figure 3, Table S3). Total N was also the most
313 important predictor of R_s considering healthy trees separately (Figure 3, Table S3), but it was
314 not a good predictor for the R_s under affected and dead trees, which shared labile C as one of
315 their most important predictors. Bulk density and T_{soil} were the second and third most important
316 predictors of R_s under affected trees, whereas, under dead trees, T_{soil} and SWC occupied the
317 first and the third position, respectively, explaining, along with labile C, up to 93% of the
318 variance of R_s (Table S3).
319
320 **4. Discussion**
321 *4.1 Interacting effects of year, season, and tree decline on soil microclimate and* R_s

The 16% higher annual precipitation in *year 2* compared to that in *year 1* led to higher SWC and R_s (14%) annual means. These differences in R_s between years were likely driven by not only the differences in the amount but also in the timing of precipitation between years. The rainfall events at the end of summer and in fall of 2014 are typical of these ecosystems and coincide with optimal temperature and nutrient availability conditions, promoting high microbial and plant activity rates (Birch, 1958; Jarvis et al., 2007). Contrary, *Year 1* showed the highest soil moisture conditions in winter, when temperature and biotic (plant and microbial activity are the lowest. Thus, our results support the importance of specifically considering alterations in the timing of rainfall events when assessing the effects of climate change on soil C fluxes (Rey et al., 2021). More importantly, the higher differences in R_s between years observed under healthy (22%) than under affected (5%) and dead (16%) trees suggest that tree decline modifies the response of R_s to annual changes in soil moisture conditions. These observations, based on only two years, are supported by the highest positive response of R_H to induced drying-rewetting cycles in soils collected under healthy trees observed at the same site (Rodríguez et al. 2019). Thus, our study adds new evidence that tree decline modulates the responses of soil functioning to climatic variability, suggesting that explicit consideration of tree health and precipitation distribution might improve ecosystem C balances and climate-change models.

As hypothesized, our study showed that tree decline strongly influences soil microclimatic conditions, particularly SWC, and R_s, but these effects largely depended on climatic variability. The trend toward increased maximums of T_{soil} during the whole studied period and the decrease in the values for fall 2014 with defoliation degree reflects the important role of healthy canopies in protecting the soil from large changes in air temperature (Lozano-Parra et al., 2018). Supporting previous studies (e.g. Curiel Yuste et al. 2019), tree decline had a significant positive effect on SWC with overall higher values under dead than under healthy

trees, and intermediate values under affected trees. This positive effect could be the result of enhanced accumulation of soil organic matter (i.e. litterfall inputs from both above- and belowground) but also reduced absorption and capture of water from roots and canopies, respectively (Anderegg et al., 2012; Wang et al., 2012). Although we did not find an overall effect of tree decline on R_s, we did find interesting significant interactions between tree decline and climatic variability (annual and seasonal), with higher values of R_s under healthy than under affected trees, particularly in *year 2* and in all seasons except in spring, and intermediate values under dead trees. Besides altering soil abiotic conditions, drought-induced tree decline might limit the supply of photosynthates to the radical organs and exudates and dead organic matter to soil microbial communities (e.g. Högberg et al. 2001; Barba et al. 2016). This disruption of the belowground C allocation is known to decrease R_A and R_H (Högberg et al., 2001; Nave et al., 2011), thus explaining the decrease in R_s under affected trees. However, in the case of dead trees, increases in litterfall, resource (e.g., carbon, nutrients, and light) availability, and other processes as a result of canopy losses (e.g., photodegradation and exposure to small rainfall pulses and dew; Rey et al. 2011; Gilkman et al., 2018; Wang et al. 2012) might have enhanced R_H and compensated, at least partially, the assumed decrease in R_A (e.g., Curiel Yuste et al., 2019). Indeed, Moore et al. (2013) found a tree mortality-driven initial decline in soil C efflux of subalpine forests from the Western United States, a partial recovery after about 5–6 years associated with increased incorporation of leaf litter C into soil organic matter, and a further decline in years 8–10. Although we do not know exactly when our holm oak trees died, the fact that most of the dead trees were still standing when we performed the study indicates that it occurred a short time before our sampling (< 10 years). Therefore, it is likely that our results might correspond to the temporary recovery of soil respiration under dead trees observed by Moore et al. (2013). Also, our results did not appreciably change when expressing R_s on a soil C basis, stressing the important role of soil C content and R_H, and to a

lesser extent of soil C quality and/or R_A, as drivers of that response. In a previous study on the same site, Rodríguez et al. (2017) found that while potential R_H was up to 66% lower under affected than under healthy trees, dead trees showed similar values of R_H to those of healthy trees (Rodríguez et al., 2017). Thus, although these previous results do not support the hypothesis of higher R_H under dead than under healthy trees, they do suggest a potential recovery of R_H after tree death. Although we did not analyze the different components of R_s separately, and the R_H values from Rodriguez et al. (2017) do not take into account all the climatic variability of our two-year study, all above suggest that the heterotrophic component could have a key role in the observed response of R_s to tree decline in this Mediterranean woodland.

The apparent lack of effect of forest die-off on soil C and nutrient cycling during spring could be largely explained by the herbaceous colonization under declining trees (Rodríguez et al. 2017) and the peak activity of herbaceous roots during this season, which may have helped offset the negative effect of tree decline over the tree and soil microbial activity (Avila et al., 2016; Rodríguez et al., 2019; Tang and Baldocchi, 2005). On the other hand, whereas we did not find differences in winter T_{soil} and summer SWC among decline stages, we did find them in R_s in both winters and summers, suggesting a high resilience of the R_A component to unfavorable climatic conditions in healthy but not in declining trees. In any case, our study shows that the soil effects of tree decline are detectable before tree death. Further, our results suggest that, as mortality increases in this type of woodlands, and provided that conditions for microbial functioning are met, they could still emit a significant amount of CO_2 while likely fixing much less C from the atmosphere than healthy woodlands. This situation could lead, at least in the short- (i.e. years) to medium-term (i.e. decades), to a swift in the role of these forests from sinks to sources of C (Baldocchi et al., 2004; Nave et al., 2011; Xiong et al., 2011). The strong negative effects of forest die-off on both soil C content and lability observed in this

system by Rodríguez et al. (2020) support this hypothesis. Finally, these results reinforce the need to consider both the spatial (i.e. different declining stages) and climatic (seasonal and annual) variability, two components still scarcely explored together, when trying to fully understand the complex effects of tree decline on soil attributes and functioning (Avila et al., 2016).

4.2 Effect of tree decline on the relationship of R_s with soil microclimatic conditions

As expected (e.g. Rey et al. 2011; Barba et al. 2016), R_s was better explained by T_{soil} up to a determined threshold (Period I), which corresponded with still optimal T_{soil} (~17ºC) but low SWC (< 7%) conditions. Thus, once SWC reached limiting values, R_s was no longer better explained by T_{soil} but by SWC (Period II), highlighting the key role of water availability in the functioning of Mediterranean ecosystems (Reichstein et al., 2002; Rey et al., 2011, 2002). The basal respiration values supported the lower respiration activity under affected than under healthy trees discussed above. Interestingly, the higher Q_{10} values and variances of R_s explained by T_{soil} and SWC under declining than under healthy trees, along with the significant correlations found between the seasonal means of R_s and those of precipitation only under declining trees might suggest that the control of R_s by soil microclimatic variables increases with tree decline. As autotrophic and heterotrophic respirations at the stand level are mainly controlled by plants and soil microclimate, respectively (Chen et al., 2019; Högberg et al., 2001; Matteucci et al., 2015), our results might indicate an increase in the relative contribution of the heterotrophic respiration under tree decline. In any case, these results stress the capacity of tree decline to sharply modulate the relationship of R_s with soil microclimatic variables.

4.3 Main drivers of R_s at the stand scale

Our results confirmed our third hypothesis about changes in the relative importance of plant, soil microclimatic, and physicochemical variables controlling R_s considering the tree decline stages together and separately. Our results revealed that canopy diameter (a good proxy of tree decline; see methods section) is the most important predictor of R_s, indicating that, at the stand level, healthier trees with larger canopies support higher R_s rates. These results highlight both the important role of tree decline (i.e. health status) as a driver of the ecosystem functioning and the important contribution of the autotrophic component to R_s in our ecosystem. Along with canopy diameter, total N was also a very important predictor of R_s, and the most important predictor under healthy trees, supporting the notion of N as a key nutrient for these ecosystems' functioning (Högberg et al., 2001). Furthermore, the observed negative correlation between canopy diameter and the C:N ratio (Figure S1) supports the previously observed negative effect of forest die-off on soil organic matter quality and N availability (Rodríguez et al., 2020, 2017). Altogether, these results warn about a likely positive feedback between forest die-off and N limitation (Gessler et al., 2016), with important implications for the ecosystem C and N balance.

The best models and most important predictors obtained for healthy as compared to affected and dead trees demonstrate that tree decline changes the relative importance of the different R_s, with microclimate variables gaining importance as the defoliation degree increases. Tree defoliation triggers a cascade effect on plant understory and soil microbial communities with important implications for ecosystem C and N budgets, including a decrease in soil organic matter lability (Rodríguez et al. (2017, 2020), which could largely affect R_H (Rodríguez et al., 2019; Rui et al., 2016). As discussed above, C:N ratio increased as canopy diameter decreased, supporting the negative effect of tree defoliation and mortality on soil organic matter quality. Accordingly, the best models for both affected and dead trees included labile C as one of the most important R_s predictors. Bulk density and T_{soil} were the second and

446 third most important predictors for R_s under affected trees, whereas the best model of R_s under
447 dead trees included T_{soil} and SWC as the most important predictors. Bulk density is widely
448 recognized to be negatively related to soil organic matter content (Périé and Ouimet, 2008) and
449 roots mass (Daddow and Warrington, 1983), which are among the main controls of R_H and R_A,
450 respectively. These results would agree with the above-discussed parallel decrease in R_A and
451 R_H under affected trees and almost complete substitution of R_s for R_H under dead trees. Finally,
452 whereas the best models for healthy and affected trees never surpassed 50% of the variance
453 explained, the best model for dead trees reached 93% of the variance explained with just bulk
454 density and both soil microclimatic variables as predictors. This result might suggest a
455 simplification of the control of the soil respiration process under tree decline, which could
456 jeopardize its resilience to the global change drivers, including climate change (Hong et al.,
457 2022).
458
459 **5. Conclusions**
460 Our study adds robust and novel observational evidence of interacting effects between climatic
461 variability and drought-induced tree decline on the spatial-temporal variability of R_s in
462 Mediterranean holm-oak forests. The higher responses of R_s to variations in the amount and
463 distribution of precipitation under healthy than under declining trees stress the important role
464 of tree health as a modulator of the response of R_s to soil moisture conditions. We also show
465 that tree decline strongly influences soil microclimate and R_s in these Mediterranean forests,
466 but the magnitude of this effect depends on other factors such as the declining stage (i.e.
467 affected or dead), the year, and the season. Further, our study demonstrates that tree decline
468 also changes the relative importance of the different drivers of R_s, with microclimate variables
469 gaining importance as the defoliation degree increases. Finally, our study exposed a likely
470 positive feedback between forest die-off and N limitation and a simplification of the soil

respiration process with tree decline. Altogether, our results point towards negative impacts of drought-induced tree decline on soil C content and cycling, particularly under forecasted climate change scenarios with dryer and more intense precipitation regimes. Thus, more studies investigating the joint effects of drought-induced forest die-off and climatic variability on soil respiration and its main components at different temporal and spatial scales are needed to fully understand the fate of this important ecosystem process.

Acknowledgments

This research was supported by the Spanish National Research Council (CSIC) in the JAE-doc modality co-financed by the European Social Fund (ESF), the ATLANTIS (PID2020-113244GB-C21) projects funded by the Spanish Government, the Basque Government through the BERC 2022-2025 program, and the Spanish Ministry of Science and Innovation through the BC3 María de Maeztu excellence accreditation (MDM-2017-0714). J.D. and A.R. acknowledge support from the FCT (2020.03670.CEECIND and SFRH/BDP/108913/2015, respectively), as well as from the MCTES, FSE, UE, and the CFE (UIDB/04004/2021) research unit financed by FCT/MCTES through national funds (PIDDAC). The authors are grateful to all the people that at some point helped with fieldwork, particularly to David López. Also, special thanks to Maria José Fernández Alonso and Luis Maria Carrascal for their advice on statistics.

References

Anderegg, W.R.L., Anderegg, L.D.L., Sherman, C., Karp, D.S., 2012. Effects of widespread drought-induced aspen mortality on understory plants. Conserv. Biol. 26, 1082–1090. https://doi.org/10.1111/j.1523-1739.2012.01913.x

Avila, J.M., Gallardo, A., Gómez-Aparicio, L., 2019. Pathogen-induced tree mortality interacts with predicted climate change to alter soil respiration and nutrient availability in Mediterranean systems. Biogeochemistry 142, 53–71. https://doi.org/10.1007/s10533-018-0521-3

Avila, J.M., Gallardo, A., Ibáñez, B., Gómez-Aparicio, L., 2016. Quercus suber dieback alters soil respiration and nutrient availability in Mediterranean forests. J Ecol 104, 1441–1452. https://doi.org/10.1111/1365-2745.12618

Baldocchi, D.D., Xu, L., Kiang, N., 2004. How plant functional-type, weather, seasonal drought, and soil physical properties alter water and energy fluxes of an oak–grass savanna and an annual grassland. Agricultural and Forest Meteorology 123, 13–39. https://doi.org/10.1016/j.agrformet.2003.11.006

Barba, J., Curiel Yuste, J., Martínez-Vilalta, J., Lloret, F., 2013. Drought-induced tree species replacement is reflected in the spatial variability of soil respiration in a mixed Mediterranean forest. Forest Ecology and Management 306, 79–87. https://doi.org/10.1016/j.foreco.2013.06.025

Barba, J., Curiel Yuste, J., Poyatos, R., Janssens, I.A., Lloret, F., 2016. Strong resilience of soil respiration components to drought-induced die-off resulting in forest secondary succession. Oecologia 1–15. https://doi.org/10.1007/s00442-016-3567-8

Birch, H.F., 1958. The effect of soil drying on humus decomposition and nitrogen availability. Plant Soil 10, 9–31. https://doi.org/10.1007/BF01343734

Bretz, F., Hothorn, T., Westfall, P., 2011. Multiple Comparisons Using R. CRC Press.

515 Burnham, K.P., Anderson, D.R., 2010. Model Selection and Multimodel Inference: A
516 Practical Information-Theoretic Approach, 2nd edition. ed. Springer, New York,
517 USA.
518 Carnicer, J., Coll, M., Ninyerola, M., Pons, X., Sánchez, G., Peñuelas, J., 2011. Widespread
519 crown condition decline, food web disruption, and amplified tree mortality with
520 increased climate change-type drought. PNAS 108, 1474–1478.
521 https://doi.org/10.1073/pnas.1010070108
522 Chen, Z., Xu, Y., Castellano, M.J., Fontaine, S., Wang, W., Ding, W., 2019. Soil Respiration
523 Components and their Temperature Sensitivity Under Chemical Fertilizer and
524 Compost Application: The Role of Nitrogen Supply and Compost Substrate Quality.
525 Journal of Geophysical Research: Biogeosciences 124, 556–571.
526 https://doi.org/10.1029/2018JG004771
527 Chiti, T., Certini, G., Marzaioli, F., D'Acqui, L.P., Forte, C., Castaldi, S., Valentini, R., 2019.
528 Composition and turnover time of organic matter in soil fractions with different
529 magnetic susceptibility. Geoderma 349, 88–96.
530 https://doi.org/10.1016/j.geoderma.2019.04.042
531 Curiel Yuste, J., Baldocchi, D.D., Gershenson, A., Goldstein, A., Misson, L., Wong, S., 2007.
532 Microbial soil respiration and its dependency on carbon inputs, soil temperature and
533 moisture. Global Change Biology 13, 2018–2035. https://doi.org/10.1111/j.1365-
534 2486.2007.01415.x
535 Curiel Yuste, J., Flores-Rentería, D., García-Angulo, D., Hereş, A.-M., Bragă, C., Petritan,
536 A.-M., Petritan, I.C., 2019. Cascading effects associated with climate-change-induced
537 conifer mortality in mountain temperate forests result in hot-spots of soil CO2
538 emissions. Soil Biology and Biochemistry 133, 50–59.
539 https://doi.org/10.1016/j.soilbio.2019.02.017

Daddow, R.L., Warrington, G., 1983. Growth-limiting soil bulk densities as influenced by soil texture. Watershed Systems Development Group, USDA Forest Service.

Edburg, S., Hicke, J., Brooks, P., Pendall, E., Ewars, B., Norton, U., Gochis, D., Guttman, E., Meddens, A., 2012. Cascading impacts of bark beetle-caused tree mortality on coupled biogeophysical and biogeochemical processes. Frontiers in Ecology and the Environment 10, 416–424. https://doi.org/10.1890/110173

Felicísimo, Á.M., Muñoz, J., Villalba, C.J., Mateo, R.G., 2011. Impactos, vulnerabilidad y adaptación al cambio climático de la biodiversidad española. 1. Flora y vegetación. Oficina Española de Cambio Climático, Ministerio de Medio Ambiente y Medio Rural y Marino, Madrid.

Gallardo, A., Covelo, F., Morillas, L., Delgado, M., 2009. Ciclos de nutrientes y procesos edáficos en los ecosistemas terrestres: especificidades del caso mediterráneo y sus implicaciones para las relaciones suelo-planta. Revista Ecosistemas 18. https://doi.org/10.7818/re.2014.18-2.00

García-Angulo, D., Hereş, A.-M., Fernández-López, M., Flores, O., Sanz, M.J., Rey, A., Valladares, F., Curiel Yuste, J., 2020. Holm oak decline and mortality exacerbates drought effects on soil biogeochemical cycling and soil microbial communities across a climactic gradient. Soil Biology and Biochemistry 107921. https://doi.org/10.1016/j.soilbio.2020.107921

Gessler, A., Schaub, M., McDowell, N.G., 2016. The role of nutrients in drought-induced tree mortality and recovery. New Phytol n/a-n/a. https://doi.org/10.1111/nph.14340

Högberg, P., Nordgren, A., Buchmann, N., Taylor, A.F.S., Ekblad, A., Högberg, M.N., Nyberg, G., Ottosson-Löfvenius, M., Read, D.J., 2001. Large-scale forest girdling shows that current photosynthesis drives soil respiration. Nature 411, 789–792. https://doi.org/10.1038/35081058

565 Hong, P., Schmid, B., De Laender, F., Eisenhauer, N., Zhang, X., Chen, H., Craven, D., De
566 Boeck, H.J., Hautier, Y., Petchey, O.L., Reich, P.B., Steudel, B., Striebel, M., Thakur,
567 M.P., Wang, S., 2022. Biodiversity promotes ecosystem functioning despite
568 environmental change. Ecology Letters 25, 555–569.
569 https://doi.org/10.1111/ele.13936
570 IPCC, 2021. Climate Change 2021: The Physical Science Basis. Contribution of Working
571 Group I to the Sixth Assessment Report of the Intergovernmental Panel on Climate
572 Change, Masson-Delmotte, V., P. Zhai, A. Pirani, S. L. Connors, C. Péan, S. Berger,
573 N. Caud, Y. Chen, L. Goldfarb, M. I. Gomis, M. Huang, K. Leitzell, E. Lonnoy, J. B.
574 R. Matthews, T. K. Maycock, T. Waterfield, O. Yelekçi, R. Yu and B. Zhou (eds.).
575 ed.
576 Jarvis, P., Rey, A., Petsikos, C., Wingate, L., Rayment, M., Pereira, J., Banza, J., David, J.,
577 Miglietta, F., Borghetti, M., Manca, G., Valentini, R., 2007. Drying and wetting of
578 Mediterranean soils stimulates decomposition and carbon dioxide emission: the
579 "Birch effect." Tree Physiol. 27, 929–940.
580 Liu, Y., Liu, S., Wan, S., Wang, J., Luan, J., Wang, H., 2016. Differential responses of soil
581 respiration to soil warming and experimental throughfall reduction in a transitional
582 oak forest in central China. Agricultural and Forest Meteorology 226–227, 186–198.
583 https://doi.org/10.1016/j.agrformet.2016.06.003
584 Lloret, F., Siscart, D., Dalmases, C., 2004. Canopy recovery after drought dieback in holm-
585 oak Mediterranean forests of Catalonia (NE Spain). Global Change Biology 10,
586 2092–2099. https://doi.org/10.1111/j.1365-2486.2004.00870.x
587 Lozano-Parra, J., Pulido, M., Lozano-Fondón, C., Schnabel, S., 2018. How do Soil Moisture
588 and Vegetation Covers Influence Soil Temperature in Drylands of Mediterranean
589 Regions? Water 10, 1747. https://doi.org/10.3390/w10121747

590 Matteucci, M., Gruening, C., Goded Ballarin, I., Seufert, G., Cescatti, A., 2015. Components,
591 drivers and temporal dynamics of ecosystem respiration in a Mediterranean pine
592 forest. Soil Biology and Biochemistry 88, 224–235.
593 https://doi.org/10.1016/j.soilbio.2015.05.017
594 Moore, D.J.P., Trahan, N.A., Wilkes, P., Quaife, T., Stephens, B.B., Elder, K., Desai, A.R.,
595 Negron, J., Monson, R.K., 2013. Persistent reduced ecosystem respiration after insect
596 disturbance in high elevation forests. Ecology Letters 16, 731–737.
597 https://doi.org/10.1111/ele.12097
598 Nave, L.E., Gough, C.M., Maurer, K.D., Bohrer, G., Hardiman, B.S., Le Moine, J., Munoz,
599 A.B., Nadelhoffer, K.J., Sparks, J.P., Strahm, B.D., Vogel, C.S., Curtis, P.S., 2011.
600 Disturbance and the resilience of coupled carbon and nitrogen cycling in a north
601 temperate forest. J. Geophys. Res. 116, G04016.
602 https://doi.org/10.1029/2011JG001758
603 Périé, C., Ouimet, R., 2008. Organic carbon, organic matter and bulk density relationships in
604 boreal forest soils. Can. J. Soil. Sci. 88, 315–325. https://doi.org/10.4141/CJSS06008
605 Pinheiro, J., Bates, D., DebRoy, S., Sarkar, D., R Core Team, 2020. nlme: Linear and
606 Nonlinear Mixed Effects Models. R package version 3.1-148.
607 R Core Team, 2017. R: A language and environment for statistical computing. R Foundation
608 for Statistical Computing,. Vienna, Austria.
609 Raich, J.W., Schlesinger, W.H., 1992. The global carbon dioxide flux in soil respiration and
610 its relationship to vegetation and climate. Tellus B 44, 81–99.
611 https://doi.org/10.1034/j.1600-0889.1992.t01-1-00001.x
612 Rangel, T.F., Diniz-Filho, J.A.F., Bini, L.M., 2010. SAM: a comprehensive application for
613 Spatial Analysis in Macroecology. Ecography 33, 46–50.
614 https://doi.org/10.1111/j.1600-0587.2009.06299.x

615 Reichstein, M., Bahn, M., Ciais, P., Frank, D., Mahecha, M.D., Seneviratne, S.I.,
616 Zscheischler, J., Beer, C., Buchmann, N., Frank, D.C., Papale, D., Rammig, A.,
617 Smith, P., Thonicke, K., van der Velde, M., Vicca, S., Walz, A., Wattenbach, M.,
618 2013. Climate extremes and the carbon cycle. Nature 500, 287–295.
619 https://doi.org/10.1038/nature12350
620 Reichstein, M., Tenhunen, J.D., Roupsard, O., Ourcival, J., Rambal, S., Miglietta, F.,
621 Peressotti, A., Pecchiari, M., Tirone, G., Valentini, R., 2002. Severe drought effects
622 on ecosystem CO2 and H2O fluxes at three Mediterranean evergreen sites: revision of
623 current hypotheses? Global Change Biology 8, 999–1017.
624 https://doi.org/10.1046/j.1365-2486.2002.00530.x
625 Rey, A., Carrascal, L.M., Báez, C.G.-G., Raimundo, J., Oyonarte, C., Pegoraro, E., 2021.
626 Impact of climate and land degradation on soil carbon fluxes in dry semiarid
627 grasslands in SE Spain. Plant Soil 461, 323–339. https://doi.org/10.1007/s11104-021-
628 04842-y
629 Rey, A., Oyonarte, C., Morán-López, T., Raimundo, J., Pegoraro, E., 2017. Changes in soil
630 moisture predict soil carbon losses upon rewetting in a perennial semiarid steppe in
631 SE Spain. Geoderma, STRUCTURE AND FUNCTION OF SOIL AND SOIL
632 COVER IN A CHANGING WORLD: CHARACTERIZATION AND SCALING
633 287, 135–146. https://doi.org/10.1016/j.geoderma.2016.06.025
634 Rey, A., Pegoraro, E., Oyonarte, C., Were, A., Escribano, P., Raimundo, J., 2011. Impact of
635 land degradation on soil respiration in a steppe (Stipa tenacissima L.) semi-arid
636 ecosystem in the SE of Spain. Soil Biology and Biochemistry 43, 393–403.
637 https://doi.org/10.1016/j.soilbio.2010.11.007
638 Rey, A., Pegoraro, E., Tedeschi, V., De Parri, I., Jarvis, P.G., Valentini, R., 2002. Annual
639 variation in soil respiration and its components in a coppice oak forest in Central

Italy. Global Change Biology 8, 851–866. https://doi.org/10.1046/j.1365-2486.2002.00521.x

Rodríguez, A., Chiti, T., Rey, A., Durán, J., 2020. Forest die-off reduces soil C and N content and increases C stability in a Mediterranean woodland. Geoderma 359, 113990. https://doi.org/10.1016/j.geoderma.2019.113990

Rodríguez, A., Durán, J., Rey, A., Boudouris, I., Valladares, F., Gallardo, A., Yuste, J.C., 2019. Interactive effects of forest die-off and drying-rewetting cycles on C and N mineralization. Geoderma 333, 81–89. https://doi.org/10.1016/j.geoderma.2018.07.003

Rodríguez, A., Yuste, J.C., Rey, A., Durán, J., García-Camacho, R., Gallardo, A., Valladares, F., 2017. Holm oak decline triggers changes in plant succession and microbial communities, with implications for ecosystem C and N cycling. Plant Soil 414, 247–263. https://doi.org/10.1007/s11104-016-3118-4

Rui, Y., Murphy, D.V., Wang, X., Hoyle, F.C., 2016. Microbial respiration, but not biomass, responded linearly to increasing light fraction organic matter input: Consequences for carbon sequestration. Sci Rep 6, 35496. https://doi.org/10.1038/srep35496

Schlesinger, W.H., Andrews, J.A., 2000. Soil respiration and the global carbon cycle. Biogeochemistry 48, 7–20. https://doi.org/10.1023/A:1006247623877

Schlesinger, W.H., Dietze, M.C., Jackson, R.B., Phillips, R.P., Rhoades, C.C., Rustad, L.E., Vose, J.M., 2016. Forest biogeochemistry in response to drought. Global Change Biology 22, 2318–2328. https://doi.org/10.1111/gcb.13105

Song, X., Zhu, J., He, N., Huang, J., Tian, J., Zhao, X., Liu, Y., Wang, C., 2017. Asynchronous pulse responses of soil carbon and nitrogen mineralization to rewetting events at a short-term: Regulation by microbes. Scientific Reports 7, 7492. https://doi.org/10.1038/s41598-017-07744-1

Taiyun, W., Simko, V., 2017. R package “corrplot”: Visualization of a Correlation Matrix version 0.84 from CRAN.

Tang, J., Baldocchi, D.D., 2005. Spatial–temporal variation in soil respiration in an oak–grass savanna ecosystem in California and its partitioning into autotrophic and heterotrophic components. Biogeochemistry 73, 183–207. https://doi.org/10.1007/s10533-004-5889-6

Wang, Q., He, N., Liu, Y., Li, M., Xu, li, 2016. Strong pulse effects of precipitation events on soil microbial respiration in temperate forests. Geoderma 275, 67–73. https://doi.org/10.1016/j.geoderma.2016.04.016

Wang, W., Peng, C., Kneeshaw, D.D., Larocque, G.R., Luo, Z., 2012. Drought-induced tree mortality: ecological consequences, causes, and modeling. Environmental Reviews 20, 109–121.

Warner, D.L., Bond-Lamberty, B., Jian, J., Stell, E., Vargas, R., 2019. Spatial Predictions and Associated Uncertainty of Annual Soil Respiration at the Global Scale. Global Biogeochemical Cycles 33, 1733–1745. https://doi.org/10.1029/2019GB006264

Xiong, Y., D’Atri, J.J., Fu, S., Xia, H., Seastedt, T.R., 2011. Rapid soil organic matter loss from forest dieback in a subalpine coniferous ecosystem. Soil Biology and Biochemistry 43, 2450–2456. https://doi.org/10.1016/j.soilbio.2011.08.013

Zhao, C., Miao, Y., Yu, C., Zhu, L., Wang, F., Jiang, L., Hui, D., Wan, S., 2016. Soil microbial community composition and respiration along an experimental precipitation gradient in a semiarid steppe. Sci Rep 6, 24317. https://doi.org/10.1038/srep24317

Tables

Table 1. Annual means of soil water content (SWC), soil temperature (T_{soil}), and soil respiration (R_s) for the two studied years, from June 2013 to May 2014 (*year 1*) and from June 2014 to May 2015 (*year 2*) (n = 10 in all cases). Values represent the mean ± 1SE. Bold P values represent statistically significant effects of tree decline (*De*) and year (*Y*), as well as significant interactions of both factors. Values with different letters within each year represent significant differences among decline stages (healthy, affected, and dead) and underlined values denote a significant year effect for the respective decline stage ($P < 0.05$).

		Decline stage			GLS Models		
Variable	Year	Healthy	Affected	Dead		χ^2	P
SWC (%)	*year 1*	2.9 ± 0.2b	4.3 ± 0.4ab	4.8 ± 0.4a	*De*	14.8	**<0.001**
	year 2	5.5 ± 0.3b	6.8 ± 0.5ab	7.4± 0.4a	*Y*	362.8	**<0.001**
					De x Y	0.58	0.749
T_{soil} (°C)	*year 1*	18.0 ± 0.2	18.3 ± 0.5	17.6 ± 0.3	*De*	1.27	0.529
	year 2	17.6 ± 0.2	18.0 ± 0.4	17.6 ± 0.3	*Y*	3.52	0.060
					De x Y	2.41	0.300
R_s (µmol C m^{-2} s^{-1})	*year 1*	2.66 ± 0.25	2.09 ± 0.08	2.35 ± 0.22	*De*	2.48	0.289
	year 2	3.24 ± 0.34a	2.19 ± 0.09b	2.72 ± 0.25ab	*Y*	19.1	**<0.001**
					De x Y	14.0	**<0.001**
R_s (µmol C Kg C^{-1} s^{-1})	*year 1*	1.04 ± 0.10	0.91 ± 0.09	0.90 ± 0.11	*De*	2.62	0.270
	year 2	1.26 ± 0.13	0.94 ± 0.08	1.07 ± 0.12	*Y*	42.5	**<0.001**
					De x Y	17.5	**<0.001**

Table 2. Seasonal means of soil water content (SWC), soil temperature (T_{soil}) and soil respiration (R_s) for the two studied years and all tree decline stages separately (n = 10 in all cases). Values represent the mean ± 1SE. Bold P values represent statistically significant effects of season (S), as well as significant tree decline x season (De x S) interactions. Values with different capital letters within each year and season represent significant differences among tree decline stages and values with different lowercase letters within each year and tree decline stage represent significant differences among seasons ($P < 0.05$).

	Decline stage			GLS models		
	Healthy	Affected	Dead		χ^2	P
			SWC (%)			
year 1						
Summer	0.8 ± 0.1c	0.8 ± 0.1c	0.9 ± 0.1c	De	0.54	0.763
Fall	2.2 ± 0.2Bb	3.7 ± 0.5Ab	4.3 ± 0.6Ab	S	505.3	**< 0.001**
Winter	6.7 ± 0.5Ba	7.5 ± 0.7ABa	8.8 ± 0.5Aa	De x S	42.1	**< 0.001**
Spring	2.9 ± 0.3Bb	4.5 ± 0.3Ab	4.7 ± 0.3Ab			
year 2						
Summer	0.9 ± 0.1c	0.9 ± 0.1c	0.9 ± 0.1c	De	14.4	**< 0.001**
Fall	8.2 ± 0.4Ba	9.7 ± 0.6ABa	11.1 ± 0.7Aa	S	2295.5	**< 0.001**
Winter	9.4 ± 1.0a	11.3 ± 1.2a	12.9 ± 1.0a	De x S	6.36	0.384
Spring	3.7 ± 0.4Bb	5.3 ± 0.4Ab	5.0 ± 0.3Ab			
			T_{soil} (°C)			
year 1						
Summer	29.9 ± 0.5a	30.2 ± 1.3a	30.7 ± 1.0a	De	7.72	< 0.05
Fall	17.0 ± 0.2c	17.0 ± 0.4c	16.1 ± 0.2c	S	1351.0	**< 0.001**
Winter	13.6 ± 0.3d	13.8 ± 0.6d	13.1 ± 0.4d	De x S	8.08	0.232
Spring	18.9 ± 0.3b	19.8 ± 0.6b	19.3 ± 0.5b			
year 2						
Summer	28.0 ± 0.4a	29.7 ± 0.8a	29.5 ± 0.6a	De	3.21	0.201
Fall	15.9 ± 0.1Ab	15.6 ± 0.3ABc	15.3 ± 0.2Bc	S	9630.6	**< 0.001**
Winter	7.5 ± 0.2c	7.3 ± 0.3d	6.7 ± 0.4d	De x S	29.7	**< 0.001**
Spring	16.8 ± 0.1b	17.5 ± 0.5b	17.1 ± 0.3b			
			R_s (µmol C m^{-2} s^{-1})			
year 1						
Summer	2.80 ± 0.52Aab	1.33 ± 0.10Bc	2.02 ± 0.38ABb	De	1.69	0.429
Fall	2.12 ± 0.24b	1.82 ± 0.10bc	2.11 ± 0.21b	S	68.6	**< 0.001**
Winter	2.95 ± 0.33Aa	2.17 ± 0.12ABb	2.12 ± 0.19Bb	De x S	25.9	**< 0.001**
Spring	3.24 ± 0.34a	2.71 ± 0.13a	2.98 ± 0.28a			
year 2						
Summer	2.38 ± 0.51Ab	1.18 ± 0.09Bb	2.06 ± 0.28ABb	De	16.0	< 0.001
Fall	3.95 ± 0.33Aa	2.79 ± 0.14Ba	3.46 ± 0.30ABa	S	180.6	**< 0.001**
Winter	1.77 ± 0.18Abc	1.15 ± 0.08Bb	1.28 ± 0.15Bc	De x S	13.8	**< 0.05**
Spring	3.37 0.39a	2.44 ± 0.12a	2.76 ± 0.29ab			

Figure captions

Figure 1 Temporal dynamics of soil temperature (T_{soil}), soil volumetric water content (SWC) and soil respiration (R_s) measured under the canopy of each tree decline stage (healthy, affected and dead), as well as the precipitation and air temperature (T_{air}) spanning the study period (June 2013 – May 2015). Dots and error bars represent the mean ± 1 SE (n = 10). SP = Spring; SU = Summer; AU = Autumn; WI = Winter.

Figure 2. Relationship between soil respiration (R_s) and soil temperature (top figures, Period I) and SWC (bottom figures, Period II) for healthy (a, d), affected (b, e) and dead (c, f) trees, respectively, using averaged values for each temperature degree. The black solid line and the dashed grey lines represent the fitted regression and the 95% confidence interval, respectively. The adjusted R^2 (R^2_{adj}) values were used as a measure of goodness-of-fit of the models. Significant relationships are denoted by *** ($P < 0.001$) and * ($P < 0.05$). T_{soil} = soil temperature; SWC= soil water content.

Figure 3. Relative importance of tree (i.e. Canopy) and soil microclimatic (i.e. SWC and T_{soil}) and physicochemical (i.e. Labile C, TN, BD) variables as predictors of two-year average values of R_s under healthy, affected, and dead trees separately and together in a Mediterranean holm oak forest from the central part of the Iberian Peninsula. Canopy, canopy diameter; SWC, soil water content; Tsoil, soil temperature; Labile C, total carbon in the magnetic fraction; TN, total N; BD, bulk density.

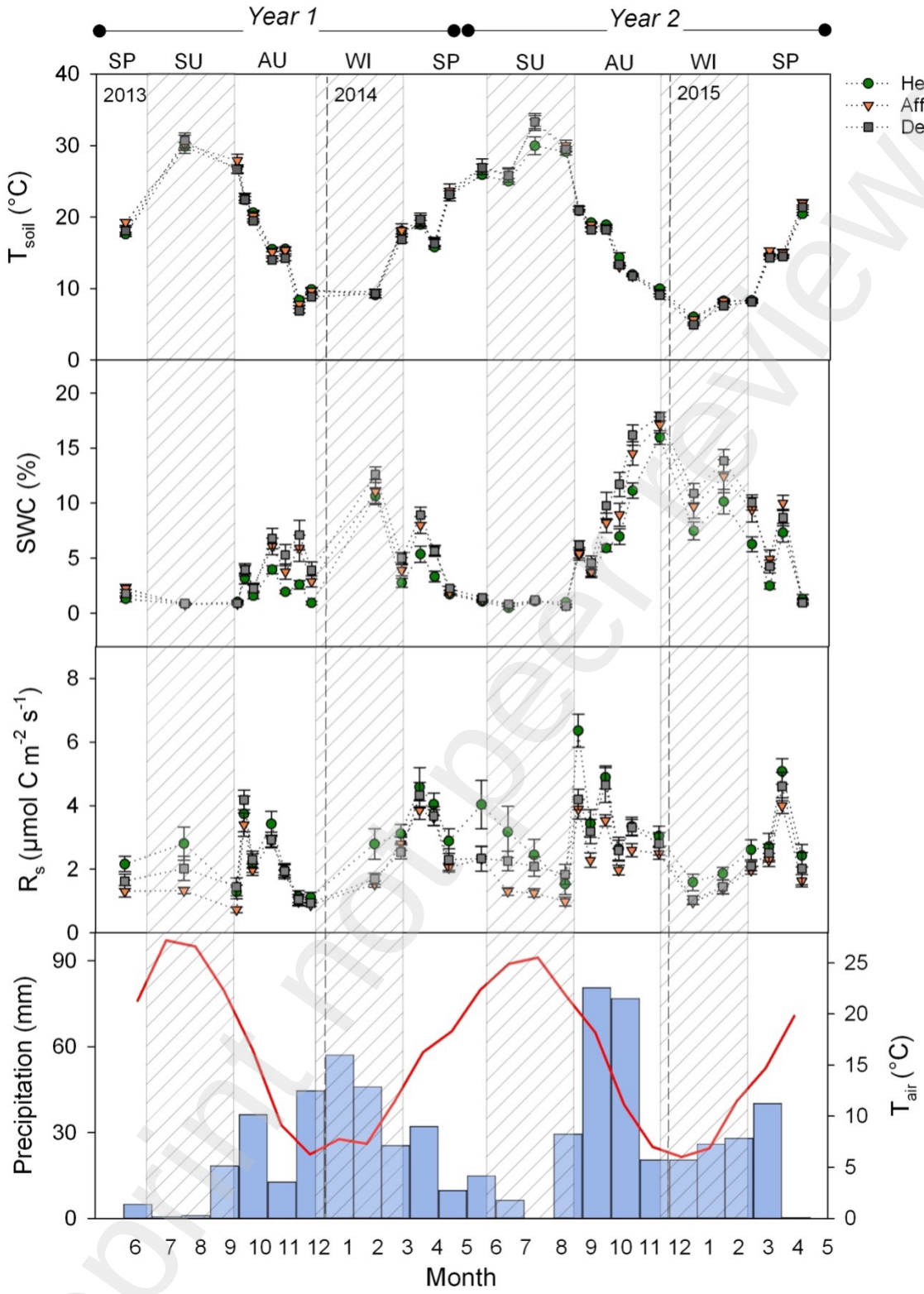

725
726 **Figure 1**

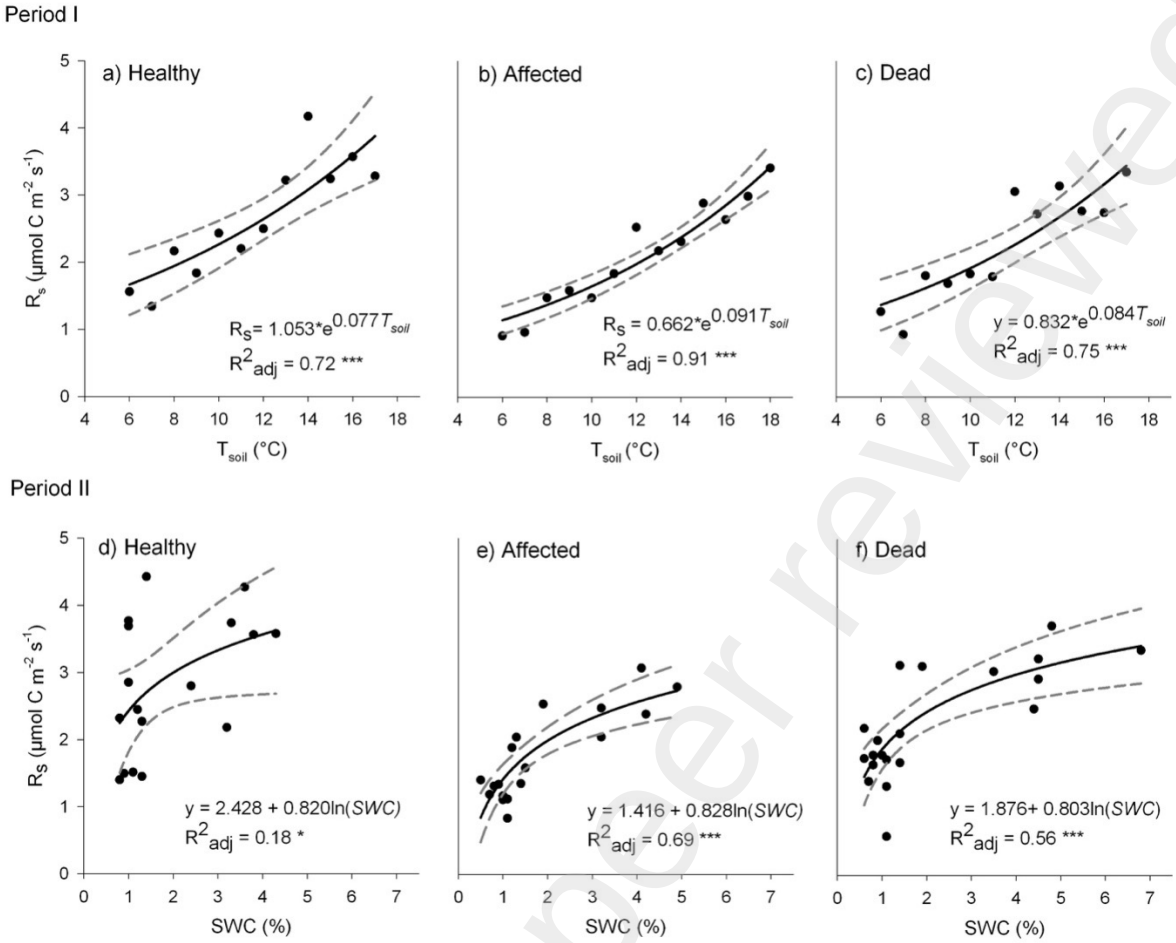

727

728 **Figure 2**

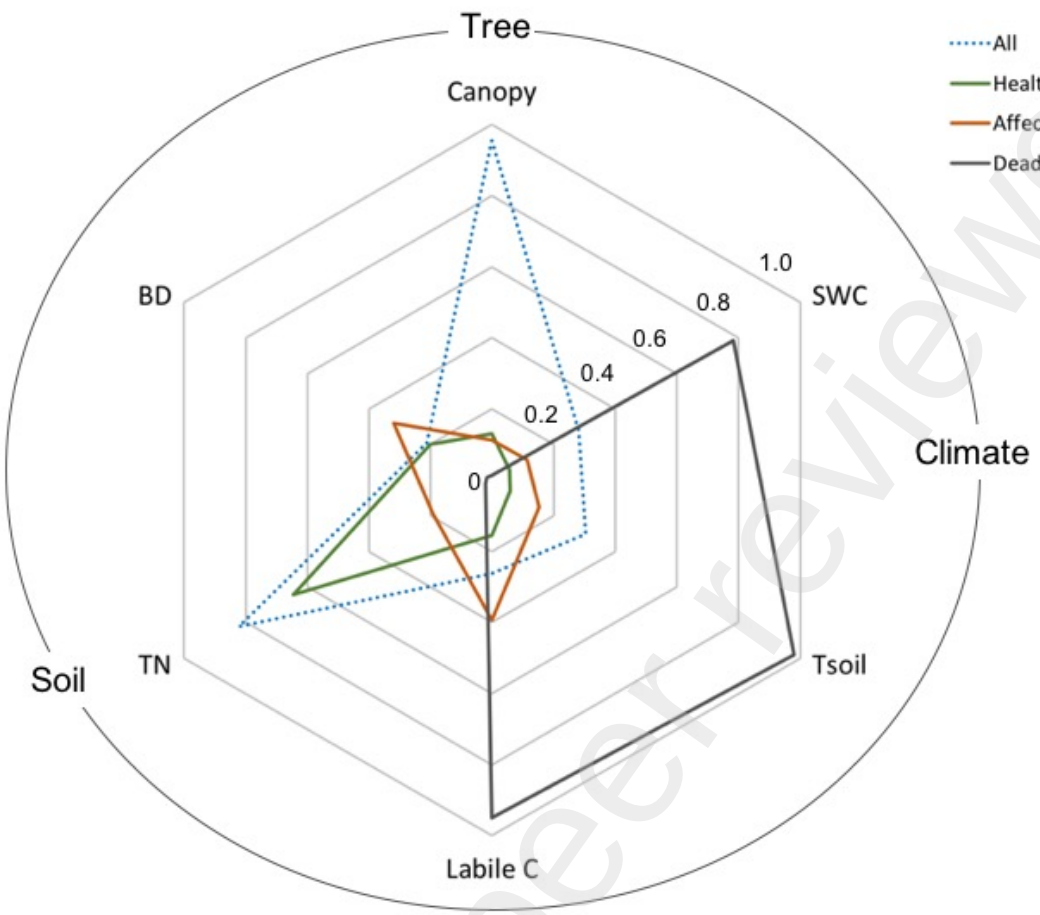

729

730 **Figure 3**

Supplementary material

Table S1. Plant structure and soil physicochemical variables for the different tree decline stages (n = 10 in all cases). Values represent the mean ± 1SE. Different letters next to values within each variable represent significant differences among defoliation degrees ($P < 0.05$; one-way ANOVA). Canopy = canopy diameter; DBH = diameter at breast height; CI = competition index; TC, total C; TN, total N; C_{MA}, total carbon in the magnetic fraction (considered as labile C). Plant variables, TC, TN, C:N ratio and pH are data from Rodríguez et al. (2017). Bulk density and C_{MA} are modified data from Rodríguez et al. (2020).

	Healthy	Affected	Dead
Plant variables			
Height (m)	4.54 ± 0.20	3.81 ± 0.15	3.82 ± 0.32
Canopy (m)	5.97 ± 0.31a	4.46 ± 0.30b	4.46 ± 0.37b
DBH (cm)	45.8 ± 3.86	33.8 ± 5.17	33.8 ± 5.17
CI (x 10^{-3})	0.8 ± 0.4a	5.5 ± 2.7ab	8.7 ± 3.3b
Soil physicochemical variables			
TC (%)	2.78 ± 0.44	2.27 ± 0.21	2.77 ± 0.31
TN (%)	0.22 ± 0.03	0.17 ± 0.02	0.21 ± 0.02
C:N ratio	12.1 ± 0.38	13.4 ± 0.43	13.1 ± 0.51
C_{MA} (%)	4.86 ± 1.07	2.79 ± 0.40	2.97 ± 0.53
pH (unitless)	6.58 ± 0.11	6.30 ± 0.10	6.56 ± 0.10
Compaction (unitless)	54 ± 15	111 ± 26	114 ± 31
Bulk density (g cm^{-3})	1.03 ± 0.08	1.09 ± 0.04	1.06 ± 0.06

Table S2. Seasonal means of precipitation (P), air temperature (T_{air}), soil water content (SWC), soil temperature (T_{soil}) and soil respiration (R_s) for the two studied years. Values represent the mean ± 1SE. Bold *P* values represent statistically significant effects of year (Y), season (S), as well as significant interactions of both factors. Values with different letters within each year represent significant differences among seasons ($P < 0.05$).

Year	Season	P (mm)*	T_{air} (°C)*	*n*	SWC (%)	T_{soil} (°C)	R_s
year 1	Summer	6.45	25.0	30	0.9 ± 0.1c	30.3 ± 0.6a	2.05 ± 0.24c
	Fall	67.3	16.0	30	3.4 ± 0.3b	16.7 ± 0.2c	2.02 ± 0.11c
	Winter	147.7	7.10	30	7.7 ± 0.4a	13.5 ± 0.3d	2.41 ± 0.15b
	Spring	67.3	15.3	30	4.0 ± 0.2b	19.3 ± 0.3b	3.03 ± 0.16a
year 2	Summer	21.2	24.3	29	0.9 ± 0.1c	29.1 ± 0.4a	1.87 ± 0.21c
	Fall	186.8	17.0	29	9.6 ± 0.4a	15.6 ± 0.1c	3.40 ± 0.17a
	Winter	66.8	6.6	29	11.1 ± 0.7a	7.2 ± 0.2d	1.40 ± 0.10d
	Spring	68.5	15.3	29	4.7 ± 0.3b	17.1 ± 0.2b	2.86 ± 0.18b
GLS models			Year	χ^2	77.8	186.2	8.07
				P	**< 0.001**	**< 0.001**	**< 0.01**
			Season	χ^2	1527.3	7142.6	218.2
				P	**< 0.001**	**< 0.001**	**< 0.001**
			Y x S	χ^2	151.7	568.6	251.5
				P	**< 0.001**	**< 0.001**	**< 0.001**

*Getafe (40°17'N 3°43'O) and Cuatro Vientos (40°22'N 3°47'O) stations (AEMET)

Table S3. Best-fitting regression models and predictors for the two-year average values of soil respiration for each tree decline stage separately (healthy, affected and dead) and all together (All). The best three models (M1-M3), ranked according to their AICc value, and the three most important predictors (Pred.), ranked according to their relative importance (Import) are presented. Coloured cells indicate variables that were included in a particular model (one per row). Canopy, tree canopy diameter; SWC, soil water content; Lab C, labile C; TN, soil total nitrogen; BD, bulk density.

	Best models								Best predictors	
	Canopy	SWC	T_{soil}	Lab C	TN	BD	R^2	AIC_c	Pred.	Import.
Healthy										
M1							0.49	29.4	TN	0.65
M2							0.34	31.9	BD	0.20
M3							0.25	33.1	Lab C	0.16
Affected										
M1							0.25	6.80	Lab C	0.39
M2							0.22	7.16	BD	0.32
M3							0.09	8.72	T_{soil}	0.15
Dead										
M1							0.93	19.7	T_{soil}	0.98
M2							0.77	23.1	Lab C	0.95
M3							0.38	26.8	SWC	0.78
All										
M1							0.42	60.9	Canopy	0.96
M2							0.45	62.5	TN	0.82
M3							0.44	62.6	T_{soil}	0.30

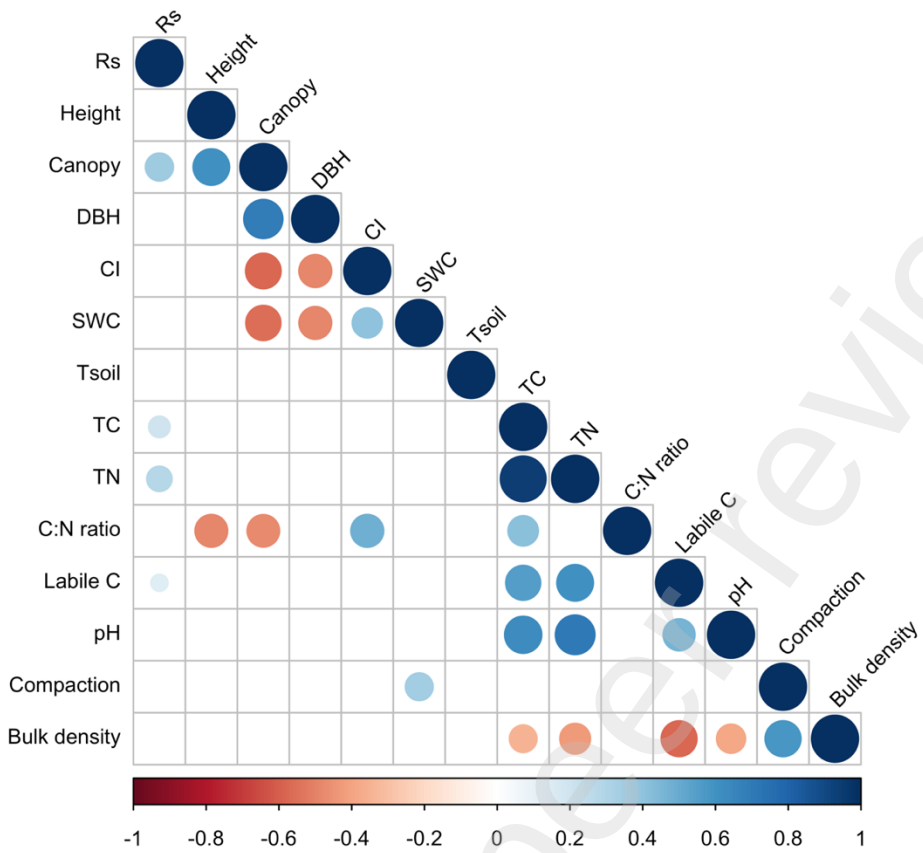

Figure S1. Heatmap representation of Spearman's rank correlation matrix among the two-year average values of soil respiration (R_s), plant (Height, Canopy, DBH, CI), and soil microclimatic (SWC and T_{soil}) and physicochemical (TC, TN, C:N ratio, Labile C, pH, Compaction, Bulk density) variables for all decline stages together. Only significant values are shown ($P < 0.05$). SWC, two-years average values of soil volumetric water content; T_{soil}, two-years average values of soil temperature; TC, total C; TN, total N.

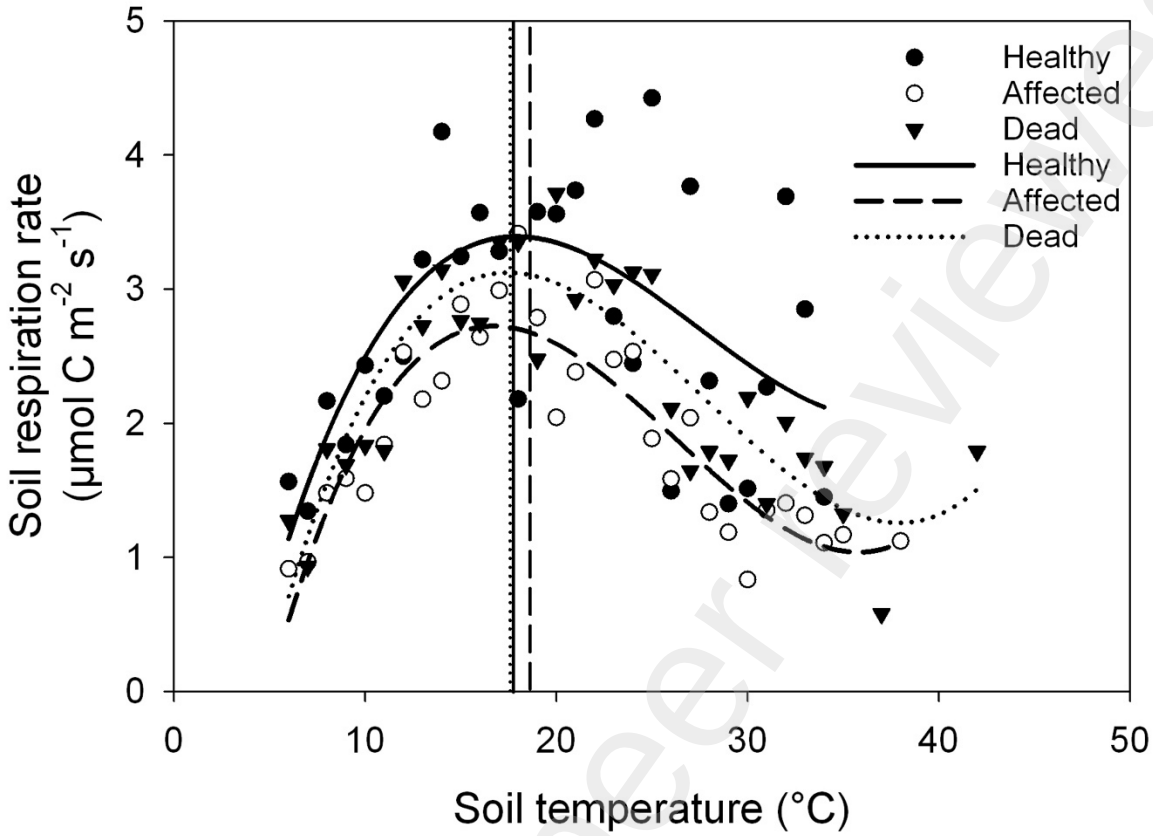

760

761 **Figure S2.** Relationship between soil temperature and soil respiration for each tree decline
762 stage using averaged values for each temperature degree. Vertical lines show the temperature
763 threshold for each decline stage (i.e., 17°C for healthy and dead and 18°C for affected).